

nearly linear. Further inspection of the figures suggests that the reduction in Nusselt number because of blowing is greater when the molecular weight of the injected gas is lower. However, there are exceptions to this relationship. In particular, in the range of small and moderate blowing rates, the Nusselt numbers corresponding to helium injection lie above those corresponding to water vapor injection. Thus, helium is a less effective coolant, and water vapor is a more effective coolant than might have been expected on the basis of a simple molecular-weight rule. Also, argon and carbon dioxide are somewhat out of order in their effect on Nusselt number, but this is of little practical importance.

The nonlinear variation of the helium results and the interchange of position between the curves for helium and water vapor has been reported previously for stagnation flow.<sup>4</sup> By making comparisons between Figs. 1 and 2, one sees only slight differences in detail; the general trends are identical.

The dashed lines appearing in the figures represent the correlation of Gross and co-workers.<sup>3</sup> The original correlation did not take account of thermal diffusional effects. However, it can be extended to include these effects by replacing  $q$  with  $h$ ; in the correlation equation thus

$$h/h_0 = 1 - [1.82/(C^*)^{1/2}][(M_2/M_1)^{1/3}(\dot{m}/\rho_\infty U_\infty)Re_x^{1/2}] \quad (4)$$

where

$$C^* = \rho^* \mu^* / \rho_\infty \mu_\infty \quad (4a)$$

and  $M_2$  and  $M_1$  denote the molecular weights of air and of the injected gas, respectively. It is evident that  $h_0$  represents the heat-transfer coefficient for no mass injection. The quantity  $C^*$  is a correction for variable fluid properties;  $\rho^*$  and  $\mu^*$  represent air properties corresponding to a reference temperature  $T^*$  that, in the absence of aerodynamic heating, is the average of  $T_w$  and  $T_\infty$ .

It is evident that the correlation equation [Eq. (4)] provides a heat-transfer coefficient that decreases linearly with increasing blowing rate. Furthermore, the correlation predicts a greater decrease in  $h$  when the molecular weight is lower.

In view of Figs. 1 and 2, it is clear that the present results are in accord with certain aspects of the correlation equation. However, the correlation does not predict the nonlinear behavior of the helium results. Furthermore, it overpredicts the reduction in heat transfer caused by helium injection and underpredicts the reduction caused by water vapor injection.

The adiabatic wall temperature results calculated as part of the present investigation are presented in Fig. 3. As was noted earlier, the adiabatic wall temperature differs from  $T_\infty$  because of the effect of diffusion thermo. Thus,  $T_{aw}$  enters the heat-transfer computation through the definition of  $h$  [Eq. (1)]. Inspection of Fig. 3 shows that, for injected gases having molecular weights exceeding the mainstream gas (air),  $T_{aw}/T_\infty \leq 1$ ; the opposite is true for injected gases lighter than air. For the very light gases, hydrogen and helium, the difference between  $T_{aw}$  and  $T_\infty$  becomes substantial at higher blowing rates. On the other hand, for the heavier gases, there is little difference between  $T_{aw}$  and  $T_\infty$ .

**References**

<sup>1</sup> Sparrow, E. M., Minkowycz, W. J., and Eckert, E. R. G., "Diffusion-thermo effects in stagnation-point flow of air with injection of gases of various molecular weights into the boundary layer," *AIAA J.* **2**, 652-659 (1954).  
<sup>2</sup> Mason, E. A. and Monchick, L., "Survey of the equation of state and transport properties of moist gases," *1963 International Symposium on Humidity and Moisture* (National Bureau of Standards, Washington, D. C., May 1963).  
<sup>3</sup> Gross, J. F., Hartnett, J. P., Masson, D. J., and Gazley, C., Jr., "A review of binary laminar boundary-layer characteristics," *Intern. J. Heat Mass Transfer* **3**, 198-221 (1961).  
<sup>4</sup> Sparrow, E. M., "Recent studies relating to mass transfer cooling," *Proceedings of the 1964 Heat Transfer and Fluid Mechanics Institute* (Stanford University Press, Stanford, Calif., 1964), pp. 1-18.

## Effects of Suction and Blowing on Oscillatory Boundary Layers over Cylinders

WEN-JEI YANG\*

*University of Michigan, Ann Arbor, Mich.*

**B**ECAUSE of the importance of the boundary-layer control, there have been extensive studies on the steady, laminar, boundary layer with suction or blowing. Recently, considerable attention has been focused on the oscillatory boundary layers induced by the acoustic waves, vibrations, and flow fluctuations of the periodic-type transients.<sup>1</sup> This paper presents the effects of uniform suction and blowing on the permanent alterations in both the wall shear stress and heat-transfer rate. The alterations are caused by the fluctuations in the magnitude and direction of the freestream velocity, the rotational oscillations of the cylinder surface, the standing waves, and the progressive waves superimposed in an otherwise forced convection field. The analysis is restricted to the quasi-steady state, which may approximate the behaviors of low-frequency fluctuations.

The fundamental equations for unsteady boundary layers have been deduced for two dimensional flow [Ref. 1, Chap. 7, Eqs. (13) and (135)]. Let  $u$  and  $v$  be the velocity components in the  $x$  and  $y$  directions, respectively;  $t$ , the physical time;  $x$  and  $y$ , the distances measured along and normal to the cylinder surface, respectively;  $p$ , the pressure;  $T$ , the fluid temperature; and  $U$ , the velocity of potential flow. The boundary conditions are  $y = 0$ :  $u = 0, v = V, T = T_w$ ;  $y = \infty$ :  $u = U, T = T_\infty$ , where  $V$  is the velocity of uniform suction for negative value and uniform blowing for positive value;  $T_w$ , the temperature of cylinder surface; and  $T_\infty$ , the fluid temperature of freestream.

Let  $U_0(x)$  be the velocity of the potential flow at steady state and  $\epsilon U_1 \cos \omega t$  be the periodic disturbance, where

$$U_0(x) = U_\infty \sum_{k=0}^{\infty} a_{2k+1} x^{2k+1}$$

$$U_1(x) = U_\infty \sum_{k=0}^{\infty} b_{2k} x^{2k}$$

$\epsilon U_1$ , the amplitude of the disturbance;  $\epsilon$ , a small constant parameter;  $\omega$ , the circular frequency; and  $a_{2k+1}$  and  $b_{2k}$  are the coefficients depending upon the geometrical configuration of the cylinder and the nature of disturbance, respectively. If the disturbance is superimposed on the freestream in the form of flow perturbations, then  $U(x, t)$  may be expressed as  $U_0(x) + \epsilon U_1(x) \cos \omega t$ . It is called the flow oscillation for  $U_0 = U_1$  and the fluctuating circulation for  $U_0 \neq U_1$ . Other disturbances, which may be superimposed on the freestream, include standing waves and progressive waves. Two typical cases of standing waves are  $\epsilon A \sin(2\pi/\lambda)x \cos \omega t$  for the nodal point of the wave coinciding with the forward stagnation point and  $\epsilon A \cos(2\pi/\lambda)x \cos \omega t$  for the point of maximum amplitude coinciding with the forward stagnation point, where  $\epsilon A$  is the magnitude, and  $\lambda$  is the wavelength of the standing waves. By including  $A \sin(2\pi/\lambda)x$  or  $A \cos(2\pi/\lambda)x$  as  $U_1(x)$ , the disturbances caused by the standing waves and freestream perturbations may be treated simultaneously. The progressive wave may be expressed as  $\epsilon A \sin[(\omega x/U_w) \mp \omega t]$ , which represents an infinite train of harmonic waves of frequency  $\omega$  and amplitude  $\epsilon A$  traveling in the positive or negative direction of  $x$  with a velocity  $U_w$ . By rewriting in the form of  $\epsilon A \sin(\omega x/U_w) \cos \omega t - \epsilon A \cos(\omega x/U_w) \sin \omega t$ , the

Received February 8, 1965; revision received April 5, 1965.  
 \* Assistant Professor, Department of Mechanical Engineering.

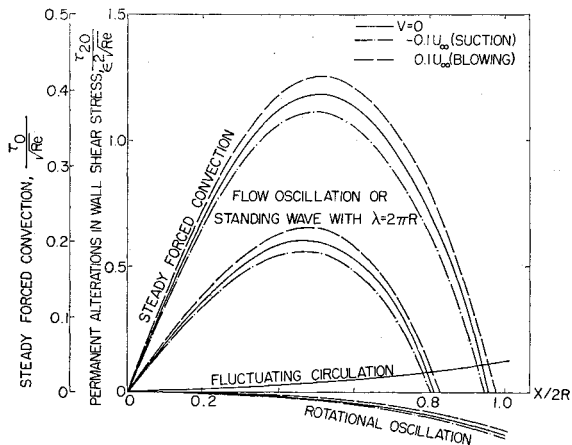


Fig. 1 Effects of the uniform suction and blowing on the steady-state components of wall shear stress.

progressive wave may be considered as the superposition of two standing waves with 90°-phase difference.

If the disturbance of the boundary layers is caused by the rotational oscillation of the cylinder surface, then  $U = U_0(x)$ , and the boundary condition  $u = 0$  at  $y = 0$  has to be replaced by  $u = \epsilon U_1 \cos \omega t$  at  $y = 0$ .

Now the velocity and temperature perturbations at quasi-steady state are taken in the same form as

$$u = u_0 + \epsilon u_1 \cos \omega t + \epsilon^2 (u_{20} + u_{21} \cos 2\omega t) + O(\epsilon^3) + \dots$$

Substituting these expressions into the fundamental equation, equating each coefficient to zero, and multiplying the ascending powers of  $\epsilon$ , one obtains a series of systems of equations, one for each of the successive approximations  $u_0, v_0, T_0; u_1, v_1, T_1$ ; etc. All of the solutions are obtained in the form of the Blasius series. The zeroth-order perturbation is the case of steady forced convection.<sup>2</sup> The first-order perturbation is the frequency response of the fluid velocity and temperature. The second-order solutions consist of the steady and periodic components. The steady components  $u_{20}, v_{20}$ , and  $T_{20}$  express the permanent alterations in velocity and temperature. They give rise to a net change in the steady values of the wall shear stress  $\tau_{20}$  and Nusselt

number  $N_{U_{20}}$ , which are obtained as

$$\frac{\tau_{20}}{\epsilon^2 (Re)} = \frac{3b_0 b_2}{2(a_1)} \left\{ f_{2011}'' + \frac{a_3 b_0}{a_1 b_2} f_{2012}'' \right\} x + \frac{2a_3}{a_1} \left\{ f_{2031}'' + \frac{a_3 b_0}{a_1 b_2} \times \right. \\ \left. f_{2032}'' + \frac{a_1 b_2}{a_3 b_0} f_{2034}'' + \frac{a_1 b_4}{a_3 b_2} f_{2034}'' + \frac{a_5 b_0}{a_3 b_2} f_{2035}'' \right\} x^3 + \dots \Bigg|_{\eta=0}$$

$$\frac{N_{U_{20}}}{\epsilon^2 (Re)} = \frac{3b_0 b_2}{2a_1^2} \left\{ F_{2001}' + \frac{a_3 b_0}{a_1 b_2} F_{2002}' + \frac{2a_3}{a_1} \left[ F_{2021}' + \frac{a_1 b_2}{a_3 b_0} \times \right. \right. \\ \left. \left. F_{2022}' + \frac{a_3 b_0}{a_1 b_2} F_{2023}' + \frac{a_1 b_4}{a_3 b_2} F_{2024}' + \frac{a_5 b_0}{a_3 b_2} F_{2025}' \right] \right\} x^2 + \dots \Bigg|_{\eta=0}$$

respectively, where  $Re$  is the Reynolds number;  $\eta$ , the distance defined as  $y(a_1 Re)^{1/2}$ ; and  $f(\eta)$  and  $F(\eta)$ , the universal functions. The equations and their appropriate boundary conditions, which define the universal functions (too many in number to be presented here), are solved by an IBM 7090 digital computer.<sup>3,4</sup>

Numerical results are obtained for the case of a uniform flow about an infinite circular cylinder. The external potential flow is  $U_0 = 2U_\infty \sin(x/R)$ , where  $U_\infty$  is the freestream velocity at infinity, and  $R$  is the radius of the cylinder. The disturbances superimposed on the system include 1) the flow oscillation with an amplitude of  $\epsilon U_0$ , 2) the fluctuating circulation caused by an alternating vortex at infinity with an amplitude of  $\epsilon U_1 = \epsilon U_\infty$ , 3) the standing wave with a wavelength  $\lambda = 2\pi R$ , whose nodal point coincides with the forward stagnation point, and 4) the rotational oscillation of the cylinder surface with an amplitude of  $\epsilon U_1 = \epsilon U_\infty$ .

The effects of the uniform suction and blowing on the steady-state components of wall shear stress and heat-transfer rate are illustrated in Figs. 1 and 2. It is disclosed from these figures that the uniform suction contributes to a decrease in both the wall shear stress and heat-transfer rate in the steady, laminar, boundary layers. The fluctuations in the boundary layers induce small permanent alterations: an increase in  $\tau_{20}$  (except that caused by the rotational oscillation of the cylinder surface, which decreases  $\tau_{20}$ ) and a decrease in  $N_{U_{20}}$ . In the forward portion of the cylinder, the superposition of the uniform suction on the oscillatory boundary layer results in 1) a decrease in both  $\tau_{20}$  and the absolute magnitude of  $N_{U_{20}}$  if the disturbance is either the flow oscillation or standing wave with the wavelength of  $2\pi R$ , 2) an increase in the absolute magnitudes of both  $\tau_{20}$  and  $N_{U_{20}}$  if the disturbance is the rotational oscillation, and 3) no appreciable variation in  $\tau_{20}$ , but a slight increase in the absolute magnitude of  $N_{U_{20}}$  if the disturbance is the fluctuating circulation. The uniform blowing of the boundary affects the permanent alterations  $\tau_{20}$  and  $N_{U_{20}}$  in the opposite manner.

If the disturbance is the progressive wave because of the linearity in the equations and their appropriate boundary conditions, the solutions up to the first-order perturbation may be obtained by the superposition of the solutions to the disturbances  $\epsilon A \sin(\omega x/U_w) \cos \omega t$  and  $-\epsilon A \cos(\omega x/U_w) \sin \omega t$ . However, because of the interaction of the secondary flows induced by these two different disturbances in the outer flow, the superposition principle cannot be applied to the solutions up to the second-order perturbation. However, the same procedure as presented may be followed, although the analysis might become involved for such case.

References

<sup>1</sup> Rosenhead, L., *Laminar Boundary Layers* (Oxford University Press, Oxford, England, 1963).  
<sup>2</sup> Frossling, N., "Evaporation, heat transfer, and velocity distribution in two-dimensional and rotationally symmetrical laminar boundary-layer flow," NACA TM1432 (1958).  
<sup>3</sup> Yang, W.-J. and Izumi, T., "Influence of fluctuating circulations on the transport phenomena from cylinders including uniform suction or blowing," AIAA J. 3, 622-630 (1965).

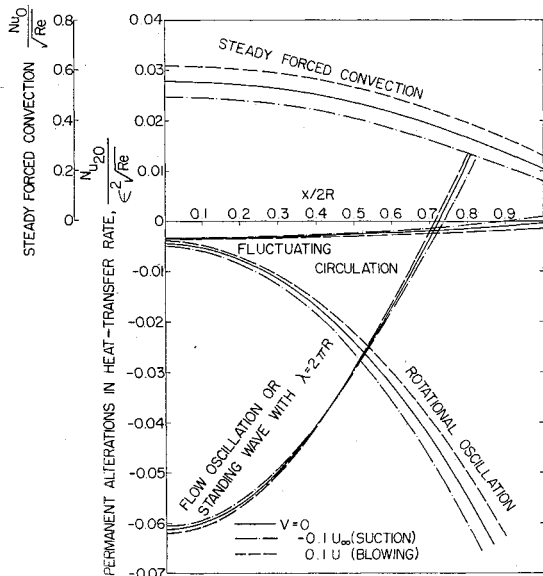


Fig. 2 Effects of the uniform suction and blowing on the steady-state components of heat transfer.

<sup>4</sup> Yang, W.-J. and Clark, J. A., "Influence of flow and rotational oscillations on the mechanics of two-dimensional laminar boundary-layer flow past cylinders including uniform suction or blowing," Univ. of Michigan, Office of Research Administration, Project 05065 (1964).

## Steadiness of a Plasmajet

EMIL PFENDER\*

University of Minnesota, Minneapolis, Minn.

AND

CLIFFORD J. CREMERS†

Georgia Institute of Technology, Atlanta, Ga.

**P**LASMAJETS generated by means of electric arcs have attracted wide scientific and technological interest during the past decade. In spite of the widespread application of plasmajets, there is still little agreement of the temperatures and temperature distributions reported by different authors. One of the reasons may be found in fluctuations of the plasmajet.

A possibility exists that the temperatures reported for turbulent plasmajets might be too high. This is because the arc column in these cases may come out of the nozzle, make a hairpin turn, and attach to an interior or exterior wall in the neighborhood of the nozzle exit. This would be an intermittent process since the arc probably travels up and out of the nozzle, extinguishes, restrikes in the nozzle, and repeats the process. Such shapes of arcs in flowing gases have been clearly detected on simpler geometries<sup>1</sup> and are presently being studied in the Heat Transfer Laboratory of the University of Minnesota. Dooley et al.<sup>2</sup> call this effect the "blown arc," which has been investigated in a similar plasma torch with a segmented anode by Wheaton and Dean.<sup>3</sup> A more recent paper by Krülle<sup>4</sup> describes experiments with a nozzle-shaped anode. Brückner<sup>5</sup> shows photographs of a 300-amp turbulent

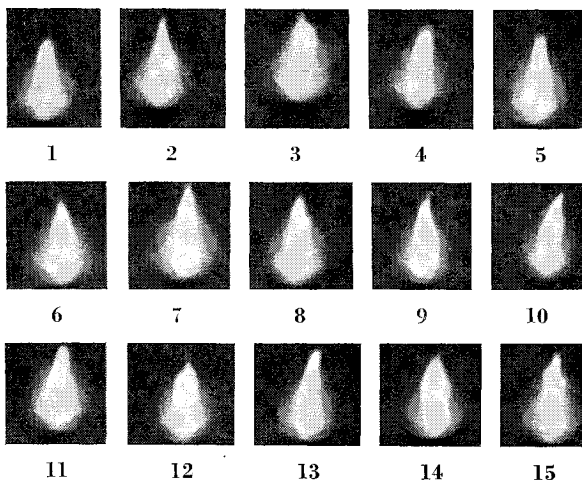


Fig. 1 High-speed Fastax pictures from an argon plasmajet, F-40 plasma torch:  $I = 400$  amp,  $P = 1$  atm, flow rate = 150 scfh.

Received March 2, 1965; revision received March 25, 1965. This work was sponsored by the Office of Aerospace Research under Contract No. AF 33(657)-7380.

\* Associate Professor of Mechanical Engineering. Member AIAA.

† Assistant Professor of Mechanical Engineering. Member AIAA.

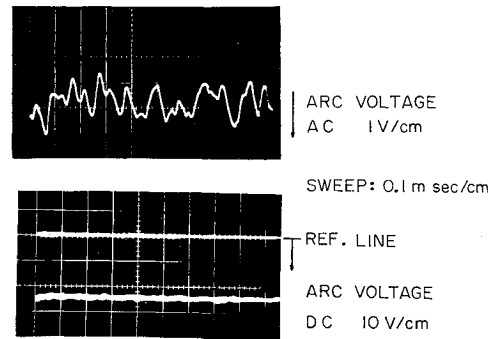


Fig. 2 Oscillograms taken of a turbulent argon jet:  $I = 400$  amp, flow rate = 150 scfh.

plasmajet in which the plasma is shown leaving the nozzle in "blobs." A photo with an exposure time of  $\frac{1}{500}$  sec shows two such entities.

If such an occurrence takes place, then the line and continuum intensities recorded would be higher than one should expect for the prevalent freestream gas temperature, since the detectors would see the very hot arc column on a high-frequency intermittent basis. The frequency would be on the order of 1 kc and so would not appear as a fluctuation in a relatively slow response detector-amplifier system. The magnitude of the effect would depend on how much of the arc column's lifetime was spent outside the nozzle.

Actually this effect could not be observed with the F-40 plasma torch<sup>†</sup> using argon as working fluid. High-speed Fastax pictures taken of the plasmajet (Fig. 1) as well as the behavior of the arc voltage (Fig. 2) did not indicate this type of fluctuation. The smooth traces of the small voltage fluctuations with a maximum amplitude of about 2.5 v show that the arc length may indeed vary within 1 cm or so but that there is no restriking of the arc which is symptomatic for the fluctuating mode of an arc. The nozzle used for all experiments has a length of 2.5 cm. The anode arc terminus usually stays in the vicinity of the nozzle entrance close to the cathode as indicated by erosion in the entrance region of the anode nozzle. According to the observed voltage fluctuations, the anode arc terminus may travel back and forth in the nozzle, but never reaches the nozzle exit, because the additional voltage required for this distance is higher than 2.5 v. Restriking of an arc with superimposed axial flow leads to a saw-tooth shape of the voltage fluctuations because the breakdown time of the restriking arc is very small as compared to the time required for the anode arc terminus to travel downstream to the nozzle exit. These effects were studied in an open geometry, which permitted unobstructed viewing of the entire arc column.

A rod-shaped thoriated tungsten cathode was positioned with its axis parallel to the surface of a plane water-cooled anode, and a gas flow (argon) was introduced parallel to the axis of the cathode. It was thought that this geometry represents the best compromise between the situation encountered in plasma generators and the accessibility of a simple model, because the flow conditions are quite similar to those with

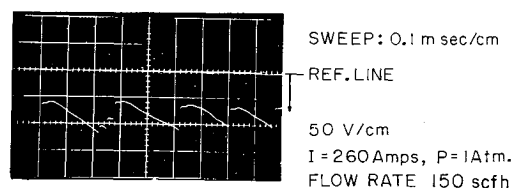


Fig. 3 Oscillogram of a nitrogen arc, F-40 plasma torch.

† Manufactured by Thermal Dynamics Corporation, Lebanon, N. H.